Solutions for Improving the Radar Refractivity Measurement by Taking Operational Constraints into Account

Lucas Besson, Jacques Parent Du Châtelet

Solutions for Improving the Radar Refractivity Measurement by Taking Operational Constraints into Account

LUCAS BESSON AND JACQUES PARENT DU CHÂTELET

Météo France, DSO/CMI, LATMOS/IPSL, Guyancourt, France

(Manuscript received 25 July 2012, in final form 6 February 2013)

ABSTRACT

Atmospheric refractivity depends on meteorological parameters such as temperature, water vapor pressure, and air pressure and can be measured using weather radar. This could be useful for convection prediction through the assimilation by numerical forecasting models in the boundary layer, particularly in prestorm conditions. However, this measurement is highly sensitive to phase ambiguities, induced by signal undersampling during rapid atmospheric fluctuations because of strong turbulent fluxes in the boundary layer or during extreme events. The refractivity measurement has been recently implemented on some radars of the French Application Radar à la Météorologie Infra-Synoptique (ARAMIS) network, which is composed of three different frequencies (S, C, and X bands). In view of operational applications, investigations are performed to improve the measurement and limit the phase ambiguity rate. The first recommendation is to decrease the time interval between two measurements by increasing the antenna speed rotation or by the use of a higher elevation angle. These methods lead to decreased sensitivity of the refractivity to the phase aliasing. The second recommendation is to improve the information from ground target by combining the two polarization radar returns and using shorter pulse width. These two different approaches, based on the radar capacity and the description of the target, are complementary and noticeably improve the quality of the refractivity retrieval.

1. Introduction

Weather radars are essential instruments for the localization and estimation of the rain rate. They are the cornerstone of monitoring and warning operational weather networks for their three-dimensional resolution and fine spatial resolution, but mostly because of their great spatial coverage. However, the occurrence of precipitation is low compared with clear-sky periods, and therefore radars are underemployed especially in terms of their potential for measurements in clear-air conditions. From these perspectives, Fabry et al. (1997) proposed to use radar echoes from ground clutter to measure the refractivity in lower-atmospheric layers. This original technique was first developed for coherent radars and is now available for noncoherent radars, which constitute most operational networks (Parent du Châtelet et al. 2012, 2007; Parent du Châtelet and Boudjabi 2008).

Weather radar refractivity presents a definite meteorological interest, particularly for studying convection initiation (Weckwerth et al. 2005; Demoz et al. 2006; Fabry 2006; Wakimoto and Murphey 2010; Bodine et al. 2010). Besson et al. (2012) showed that it can be used to characterize finescale deep convection structures. Moreover, recent studies (Montmerle et al. 2002; Sun 2005; Caumont et al. 2013) highlighted that data assimilation of weather radar refractivity into numerical weather prediction (NWP) systems can be interesting. Finally, Heinselman et al. (2009) showed that the use of refractivity fields by forecasters provided complementary information that somewhat enhanced the forecasters' capability to analyze the near-surface environment and boosted their confidence in moisture trends.

Weather radar networks are often not homogeneous. For instance, the French Application Radar à la Météorologie Infra-Synoptique (ARAMIS) operational network has three different radar frequencies (S, C, and X bands). This heterogeneity is also found with radar age (the oldest having been deployed in the mid-1980s, the newest in early 2012). These differences induce the need for an operational mode adapted to each radar; the introduction

Corresponding author address: Lucas Besson, Météo France, DSO/CMI, LATMOS/IPSL, 11 bd D'Alembert, 78280 Guyancourt, France.
E-mail: lucas.besson@latmos.ipsl.fr

DOI: 10.1175/JTECH-D-12-00167.1

of a new measurement technique should take into account the heterogeneity.

Moreover, refractivity measurements must not affect the main application for radars and restrict the reflectivity, the Doppler wind, and polarimetric measurements. To deploy refractivity measurement on operational networks, it is therefore necessary to study the link between operational modes and the quality of the refractivity retrieval and to highlight different strategies to improve and achieve the best possible measurement, within operational constraints, while reducing aliasing problems and increasing measurement accuracy.

Section 2 presents the principle of the radar refractivity retrieval and a description of the radar dataset used. Section 3 describes the tools developed and used to identify and qualify the usable ground targets for the measurement. How to improve the refractivity measurement by decreasing the sampling time is analyzed in section 4, while techniques to improve the quality of the signal from ground targets are studied in section 5. Finally, section 6 provides conclusions and perspectives.

2. Refractivity retrieval and radar data

a. Refractivity measurement

The refractivity N depends on three meteorological parameters: temperature T (K), water vapor pressure e (hPa), and air pressure P (hPa) (Bean and Dutton 1968). At the microwave frequencies, the relationship is (Smith and Weintraub 1953)

$$N = 77.6\frac{P}{T} + 3.73 \times 10^5 \frac{e}{T^2}. \quad (1)$$

The concept proposed by Fabry et al. (1997) takes advantage of the ground target returns to estimate the refractivity between the radar and the target or between two targets along the same direct electromagnetic path. The path-averaged refractivity change δN between two consecutive plan position indicators (PPIs), derived from a ground target phase change $\delta\phi$, is derived as

$$\delta\phi = \frac{4\pi f r 10^{-6}}{c}\delta N, \quad (2)$$

where f is the radar frequency (Hz), r the integration range between the radar and the target (m), and c the speed of light in a vacuum ($\mathrm{m\,s^{-1}}$).

This was initially developed for coherent radars, which operate at a constant frequency. However, most radar networks are composed of noncoherent radars, for which the frequency can drift with time. Parent du Châtelet et al. (2012, 2007) and Parent du Châtelet and Boudjabi (2008) have demonstrated that the correction to take into account the frequency variation mainly depends on the well-known local oscillator frequency and not on the transmitter frequency. After correction, refractivity is then obtained by a simple integration of $\delta\phi$ with time.

The sampling time of underlying refractivity field, generally 5 min, is determined by the operational mode of the radar. The main issue with this measurement is aliasing problems when the time becomes too long to correctly sample the signal, which in this case is undersampled. These aliasing problems have been studied by Besson et al. (2012), who showed that it depends on the range integration, the sampling time between two measurements, and the radar frequency (it is perceptible in the S band, serious in the C band, and even more serious in the X band). The radar frequency and the range integration are fixed, thus the only way to reduce the aliasing rate consists in decreasing the sampling time.

b. Radar data

The work presented here uses different radar datasets, all obtained with the S-band radar at Nîmes in the south of France and the C-band radar at Trappes (~30 km west of Paris). These two Doppler dual-polarization radars are part of the Météo France radar network ARAMIS.

Three different datasets have been used:

1) a 3-h experiment (1300–1600 UTC 1 August 2011) with the Trappes radar using a 0.4° elevation to test the effect of the rotation speed of the antenna (from 6° to 24° $\mathrm{s^{-1}}$);
2) a 24-h experiment (1400 UTC 20 September–1400 UTC 21 September 2011) with the Nîmes radar using a 0.6° elevation to test the sampling time and the effect of the transmitted pulse length (1 and 2 μs; the antenna rotation speed was 11° $\mathrm{s^{-1}}$);
3) a 24-h experiment (22 February 2012) with the Trappes radar to test the feasibility of refractivity measurements using two different interlaced elevations (i.e., 0.4° and 0.8°).

It is important to note that, in the present work, signal power is not corrected from the $1/r^2$ range effect. The power is given in decibels and not in decibels of reflectivity, the noise level is about 4 dB, and the radar of Nîmes is subject to saturation for the closest ground targets.

3. Ground targets selections

As explained in section 2a, the concept of refractivity measurement is based on the phase change between the radar and a ground target. It is essential to correctly identify echoes from ground targets and to have an idea

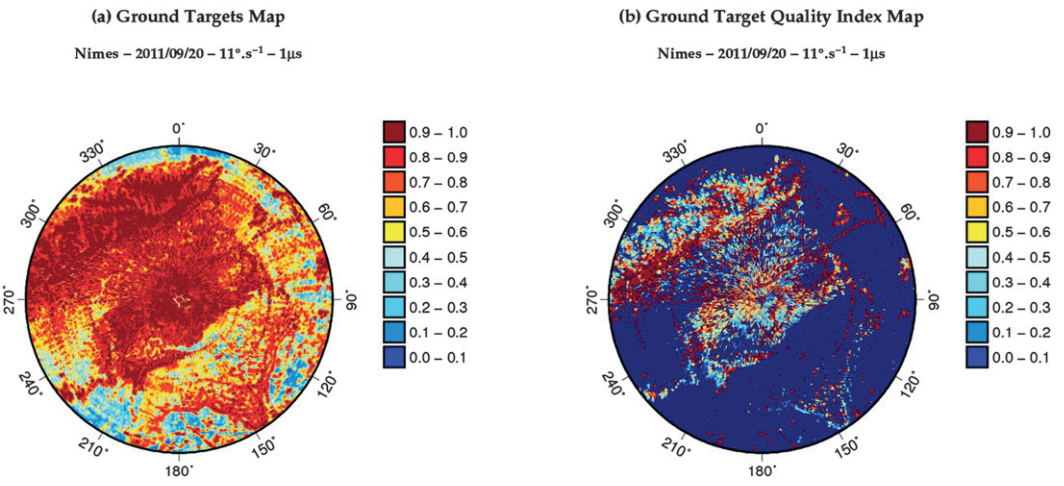

FIG. 1. Mean PPI on 20 Sep 2011 for 12-h duration around the Nîmes radar (a) for the short time signal stability σ used to select the ground pixels and (b) for the ground target quality parameter QI. The distance from the radar to the circle is 35 km, the antenna's rotation speed is 11° s^{-1}, and the pulse duration is 1 μs.

about the "quality" of these echoes. Indeed, anthropic targets generally provide a good refractivity measurement while vegetation presents a lower quality (Fabry et al. 1997; Fabry 2004). In this section, how a ground target is selected and how its quality is estimated is described.

a. Ground target identification

Hubbert et al. (2009a,b) have developed the clutter phase alignment (CPA) method to separate rain echoes from ground clutter in real time. Here, we use a similar approach also based on signal phase and amplitude by defining for each pixel a "short time signal stability" σ that is basically the inverse of the CPA:

$$\sigma = \frac{\langle I^2 + Q^2 \rangle_{0.5^\circ}}{(\langle I \rangle_{0.5^\circ}^2 + \langle Q \rangle_{0.5^\circ}^2)}, \tag{3}$$

where I and Q are respectively the real and imaginary parts of the signal. The terms in $\langle \cdot \rangle_{0.5^\circ}$ represent averaging over one pixel (i.e., 240 m in range and 0.5° in azimuth or ~100-ms duration with the 6° s^{-1} speed of the antenna).

A sample of a σ map is given in Fig. 1a for the Nîmes radar during a clear-air situation. The value of σ is close to 1 for ground targets, lower than 0.7 for meteorological echoes, and close to 0 for noise. A mixed echo (ground/rain) is in the range 0.7–0.9. In the following we apply a threshold of 0.9 on σ to select the ground clutter; the pixels for which σ is larger than this threshold are candidates for refractivity measurements.

b. Ground target quality index

The criterion defined in the previous subsection is used to evaluate the stability of the signal received during the integration time for a single measurement (about 100 ms), but we realized that it is not always enough. We therefore sought to define an additional quality index that allows quantifying of the risk of phase ambiguity over longer time intervals (typically 1 h). In this section, we proposed a simplistic quality index based on the phase change $\delta\phi$ [defined in Eq. (2)] between two successive PPIs scans (δt).

Using a large number n of phase measurements separated by δt, the quality index (QI) is defined as follows for each pixel:

$$\mathrm{QI} = \left[\left(\frac{n_{\pi/2}}{n} \right) \times 2 \right] - 1, \tag{4}$$

where $n_{\pi/2}$ is the number of time with $|\delta\phi| \leq \pi/2$. The QI is normalized by the number of samples ($1/n$) of the studied period. Even if negative values are theoretically possible, QI is generally between 0 (totally noncoherent echoes with $\delta\phi$ uniformly distributed between $-\pi$ and $+\pi$) and 1 (totally coherent echoes). In the QI map example, presented in Fig. 1b for the Nîmes radar, high-QI areas are observed (particularly in the northwest part of the figure) but also areas of low QI are observed (particularly in the southeast part of the figure), all located in ground target areas (Fig. 1a). To get a better understanding of the relative amount of pixels available for refractivity measurement, the distribution of QI is plotted in Fig. 2 for all the echoes selected as ground targets. It clearly appears that this distribution is bimodal, with a first group between −1 and 0.8 and a relatively sharp peak between 0.9 and 1. This last peak (about 30% of the ground clutter pixels) corresponds to the pixels useable for refractivity. A ground echo ($\sigma > 0.9$) can therefore be

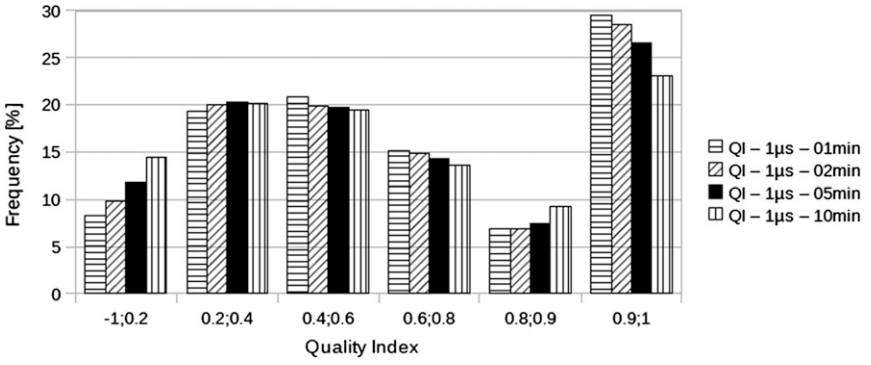

FIG. 2. QI distribution of 40 000 ground targets selected around the Nîmes radar on 20 Sep 2011 for 12 h. The horizontal hatching, diagonal hatching, solid black, and vertical hatching correspond to a 1-, 2-, 5-, and 10-min sampling time, respectively.

defined as a "good target for refractivity" if its QI is larger than 0.9; that is, the phase change after δt stays within the interval $[-(\pi/2), \pi/2]$ 95% of the time. The other ground clutter pixels (Fig. 2; QI < 0.9) frequently produce large phase changes, and they are not suitable for refractivity. Throughout the present paper, we will use the shape of the QI distribution as an indicator of the effectiveness of a number of data processing.

c. *Quality index stability with time*

Such a criterion to select "good pixels" can be used in the operational only if it is stable with time. To check this point, QI distributions are compared for two different days obtained with the Trappes C-band radar ($QI_{2011\text{-}10\text{-}15}$ for 15 October 2011 and $QI_{2012\text{-}01\text{-}01}$ for 1 January 2012). The result is shown in Fig. 3, where we have also indicated the percentage of pixels that appear at both dates in the class considered (vertical hatching). The percentage of "good targets" is similar for $QI_{2011\text{-}10\text{-}15}$ (57%) and for $QI_{2012\text{-}01\text{-}01}$ (50%; respectively, horizontal and diagonal hatching in Fig. 3). The common radar pixels (vertical hatching distribution in Fig. 3) in the highest class [0.9, 1] is close to 93%: whatever the day of QI calculation, the greatest ground targets inside the highest class remain there even several months later.

Although most pixels available for refractivity remain available whatever the season, we know that some changes may occur, like vegetation growing, buildings, and so on. It is also likely that some pixels, declared acceptable for calm propagation conditions, can become difficult to exploit during more complex propagation conditions, as in the presence of strong boundary layer turbulences. Therefore, it seems necessary to reevaluate from time to time the target selection. Even if we do not currently have enough experience to decide the frequency of this type of reassessment, it seems prudent and logical to do this every season in the temperate region.

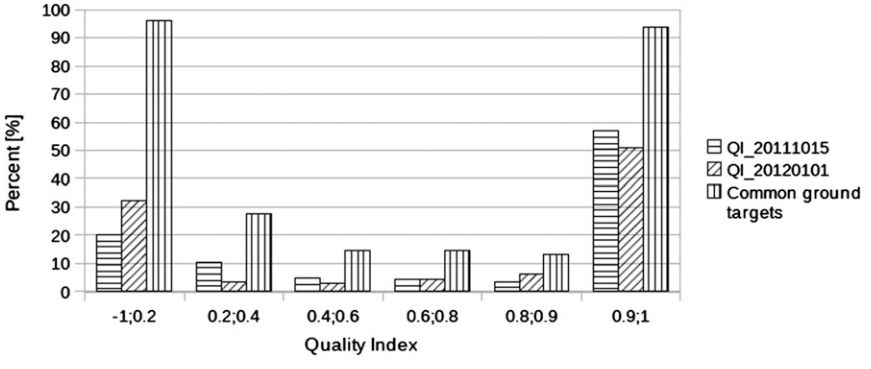

FIG. 3. QI distribution of 11 000 ground targets selected around the Trappes radar for 24 h. The horizontal hatching corresponds to the $QI_{2011\text{-}10\text{-}15}$ of 15 Oct 2011, the diagonal hatching to the $QI_{2012\text{-}01\text{-}01}$ of 1 Jan 2012, and the vertical hatching to the percentage of pixels that are present in the same class at each of the two time sequences considered.

4. Decreasing the sampling time while respecting the operational constraints

Following an extensive simulation work, Besson et al. (2012) gave an expression of the refractivity error versus the measurement conditions (sampling, frequency, range, etc.). They show that the sampling time is a critical parameter for the refractivity measurement, especially for short wavelengths (C and X bands and above) and during extreme meteorological events like deep convection or rapid atmospheric turbulences. For example, the expected aliasing rate can significantly decrease from 1.2% to 0.4% by simply reducing the sampling time by a factor of 2 (from 5 to 2.5 min with a 5-km range) for an X-band radar during an extreme convective event. In these situations, the phase change between successive measurements may be larger than π, leading to ambiguities very damaging to the measurement quality. Where applicable, an obvious solution is to reduce the sampling time. For an operational radar, which performs successive PPIs at different elevations to build periodically a complete volume scan, the sampling time for refractivity is the time it takes to make the complete volume scan, which is seldom less than 5 min.

This section focuses on the sampling time problem in an operational context: what is the sensitivity of refractivity measurement to the sampling time, how much is it sensitive to the antenna rotation speed, and is it possible to reduce the sampling time by interleaving measurements at different elevation angles?

a. Sensitivity to the sampling time

For the particular case of the Météo France radar network, the operational time sampling is 5 min. This is good enough for S-band radar and most of the time enough for the C band, but clearly too long for the X band. Using the Nîmes 24-h experiment, a statistical study is realized to evaluate the impact of changing time between two successive PPIs from 60 to 600 s. To achieve it, as the interval between two PPIs is 60 s, increasing this interval is obtained by taking 1 of 2 PPI for a sampling time of 120 s and so on, and 1 of 10 for a sampling time of 600 s. The pool of ground targets has been selected, as described in section 3a, with a QI threshold equal to 0.9, leading to a selection of approximately 40 000 pixels out of 96 480. The QI of each pixel is computed as explained in section 3b.

By focusing on the impact of the time sampling (Fig. 2), the reduction of the time between successive measurements (from 600 to 60 s) leads to an increased percentage of pixels in the higher class (i.e., [0.9, 1]) and to a decreased percentage in other classes. This improvement, significant for this calm situation, will certainly be much more important during convective or turbulent atmospheric conditions.

b. Sensitivity to the antenna speed rotation

A first option to decrease the sampling time consists in increasing the rotation speed of the antenna, but this will be at the expense of measurement accuracy, especially considering that an individual pixel is 240 m deep in distance (one gate) by 0.5° in azimuth and the number of radar pulses used in the average is inversely proportional to the antenna rotation speed: approximately 35 pulses for a rotation speed of 6° s^{-1} and only about 9 pulses at 24° s^{-1}. The test experiment, with the Trappes C-band radar, consists of realizing four successive PPIs with four different speeds (i.e., 6°, 12°, 18°, and 24° s^{-1}) for 3 h at a fixed elevation angle of 0.4°. From these data, four phase changes and refractivities are calculated for each of the selected antenna speeds.

As illustrated in Figs. 4a and 4b, for a single ground target the four time series are close to each other, confirming the low impact of the antenna rotation speed on phase change and refractivity measurements accuracy. Indeed, if a 6° s^{-1} is considered as the benchmark, the determination criterion (R^2) calculated against this reference are never lower than 0.93 for refractivity.

These observations have been generalized for all ground targets (4438), and the scores are reported in the Table 1. It can be noted that the correlation between the refractivity from the reference speed versus faster speed are good ($R^2 > 0.90$ and no bias). The decrease of R^2 depending on the rotation speed is not because of an increase of speed but to the nonsynchronization of the measurements. Indeed, between the PPI at 6° s^{-1} and the one at 24° s^{-1} a time delay of 110 s exists, leading to a significant decorrelation between measurements. To the contrary, the results are much worse for the phase differences (Table 1) with a determination coefficient close to 0.2 and a bias between 3 and 5. This is certainly due to a high-frequency noise of the phase difference time series, which is completely filtered by the integration leading to the refractivity measurement. Previous studies have shown that the phase measurement error because of the radar performance is very small, close to 6° for an individual measurement (only one radar pulse). Rapid fluctuations of the atmosphere between the radar and the target during the experiment (such as turbulent cells and cloud effects) may produce such a noise simply because the measurements are not made at the same time (see the last line of Table 1). For example, a local cooling on the order of 1°C because of a cloud above the propagation line is sufficient to explain a phase fluctuation of more than 10° (for a C-band radar with a 2-km range integration). Such changes may be coherent (between time 1.30 and 3 in Fig. 4b) or not (between time 0 and 1). The fact that the impact of rotation speed on

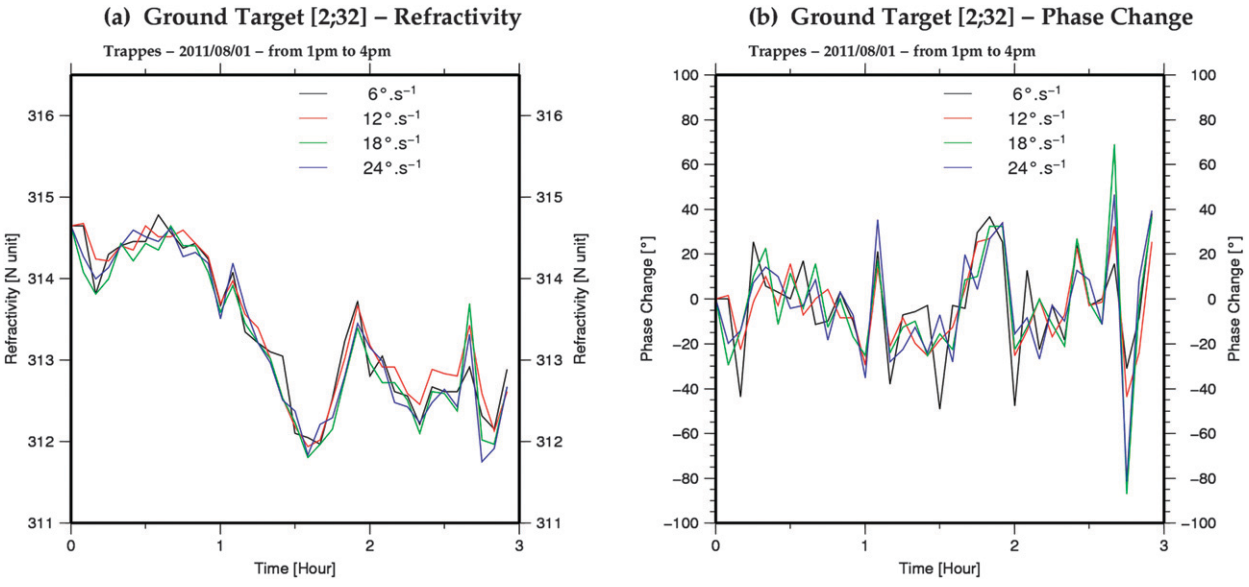

FIG. 4. (a) Refractivity and (b) 5-min phase change time series for a single ground pixel (located at 2° and ~7.5 km from the Trappes radar, gate 32), during the 3-h experiment on 1 Aug 2011 between 1300 and 1600 UTC. The corresponding rotation speeds of the antenna 6°, 12°, 18°, and 24° s^{-1} are in black, red, green, and blue, respectively.

refractivity measurement is negligible confirms previous work undertaken by Cheong et al. (2008) based on the use of phased-array radar to access a fast recovery refractivity with a low number of radar pulses.

It can be concluded that the azimuthal speed has a negligible impact on refractivity measurements. Moreover, the increase in speed is an indirect way to improve the measurement accuracy. The speed increase frees some time. With this time, more PPIs can be done at low elevations, leading to a decrease in the time between successive measurements.

c. *Interleaving of two elevation angles*

A second approach to decrease the sampling time is to use interlaced elevation angles. As the geographic positions of the radar and the target are both fixed, the optical path is strictly the same regardless of the elevation angle; the altitude reached by the beam is the same and the refractivity profiles encountered by the wave during its path remain the same. Even if the refractivity can be affected, in a general sense, by the variations of the vertical gradient of refractivity through the atmospheric propagation conditions (Park and Fabry 2010, 2011) and uncertainty (Bodine et al. 2011), this effect will not particularly be enhanced by interleaving time series from different elevation angles. However, the part of the beam that illuminates the target is not the same, and the signal amplitude should be significantly different for the two elevation angles.

To test this hypothesis, the refractivity measurement has been implemented on the C-band radar for the two interlaced elevations of 0.4° and 0.8°. The two elevations are each repeated every 5 min so that there is only 2.5 min between each elevation. Three radar refractivity time series have been retrieved with the 0.4° elevation alone (R04), with the 0.8° elevation alone (R08), and with the two elevations interleaved (R0408).

A particular ground echo, located at 2° in azimuth and at range gate 15 (~3.6 km), has been selected to evaluate the three radar refractivity time series (Fig. 5). For this target, the three different refractivities are identical, as

TABLE 1. Determination criterion and bias calculated for 4438 ground targets observed with the Trappes radar on 1 Aug 2011 for 3 h (from 1300 to 1600 UTC), according to the antenna rotation speed using a 2-μs pulse length.

	Refractivity				Phase change			
Rotation speed (° s^{-1})	6	12	18	24	6	12	18	24
Time delay between reference and measurement PPI (s)	0	60	90	110	0	60	90	110
Determination criterion (R^2)	1	0.919	0.907	0.900	1	0.297	0.235	0.200
Bias	0	−0.004	−0.004	−0.009	0	2.949	4.412	5.046

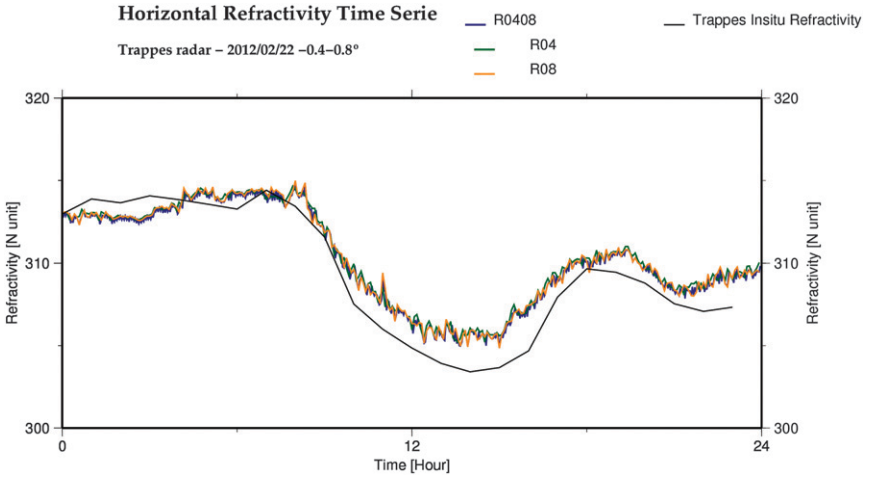

FIG. 5. A 24-h time series on 22 Feb 2012 for one selected ground target located at 2° in azimuth and at range gate 15 (~3.6 km) of the refractivity near the Trappes radar. In situ measurements at Trappes are in black. Measurements obtained for R04, R08, and R0408 are in green, orange, and blue, respectively.

confirmed by R^2 that is never lower than 0.95 (Table 2). However, it is noted (not shown) that the phase change measurement for R0408 is slightly noisier than other restitutions (R04 and R08). This is probably a result of variations in amplitude between the two elevations, which results in a change of approximately 15 dB for successive samples in the R0408 series. This strong amplitude modulation of the signal results in a frequency broadening, and thus an increase of phase noise.

The use of two successive elevation angles presents a clear advantage in view of the reduction of the sampling time, leading to a possible increase of the useful ground targets' number. A new quality index QI′, taking into account different elevation angles, can be calculated in order to evaluate the improvement brought about by this technique. This QI′ is obtained by a combination of the QI calculated with only the 0.4° elevation angle $QI_{0.4°}$, with only the 0.8° elevation angle $QI_{0.8°}$, and with the two elevation angles $QI_{0.4°-0.8°}$. Then, the QI′ is based on the best score obtained for a given ground target for the three different quality indices.

Figure 6 illustrates the improvement using two elevation angles in terms of the quality index. As expected, $QI_{0.4°-0.8°}$ presents a slightly better discrimination between good and "bad" targets than $QI_{0.4°}$ or $QI_{0.8°}$. This improvement is because of the decrease in the sampling time between successive measurements. This observation is in accordance with previous results on the time sampling illustrated by Fig. 2a. Here, the QI improvement is not very important, but, as explained by Besson et al. (2012), during extreme events or rapid fluctuations, reducing the sampling time will be very useful in order to reduce phase aliasing.

5. Two techniques to improve the retrieval quality of ground target

Section 4 was dedicated to the improvement of the refractivity measurement by decreasing the sampling time. The present section is devoted to a better use of the signal from ground targets by focusing on the influence of transmitted pulse duration and polarimetric signals.

a. Transmitted pulse duration impact on the refractivity signal

For two close targets, the received signal might be a blend of two echoes, leading to some interference. This could possibly be problematic for the refractivity restitution, especially for large pulse durations.

In this section, the dataset used is described in section 2b. The measurement is done alternatively with a 2-μs and a 1-μs pulse width. The sampling time between two PPIs with the same pulse width is about 2 min. This time sampling is chosen in order to limit the probability of phase aliasing because of too large an integration time. At first we focus on a simple signal that consists of

TABLE 2. Determination criterion and bias calculated for one selected ground target observed by the Trappes radar on 22 Feb 2012 located at 2° in azimuth and at range gate 15 (~3.6 km). Each radar refractivity has been compared to the in situ refractivity.

	R04 vs in situ	R08 vs in situ	R0408 vs in situ
Determination criterion (R^2)	0.957	0.942	0.940
Bias	0.298	0.301	0.305

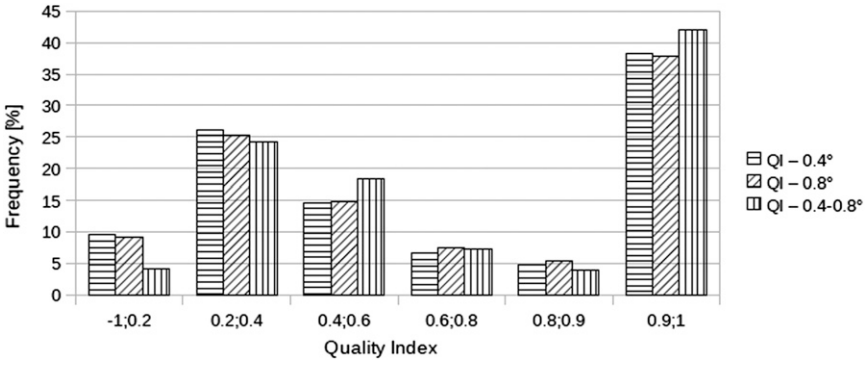

FIG. 6. QI distribution of 23 270 ground targets for 24 h selected around the Trappes radar on 22 Feb 2012. The horizontal, diagonal, and vertical hatching correspond to $QI_{0.4°}$, $QI_{0.8°}$, and $QI_{0.4°-0.8°}$, respectively.

a single isolated ground target; then we examine a more complex signal that consists of several targets blended together.

1) ISOLATED GROUND TARGET

An isolated ground target is selected in the azimuth 264° over three successive gates—110, 111, and 112—separated by 240 m corresponding to a distance from the radar of about 26.4, 26.64, and 26.88 km, respectively (Fig. 7a). As expected, the echo is more spread out with the longest pulse over the three gates for 2 μs (110, 111, and 112) and over only two gates for 1 μs (111 and 112). The corresponding refractivity time series obtained for the different gates is presented in Fig. 7c for the two pulse lengths (1 and 2 μs). The refractivities calculated are close together and have a R^2 always higher than 0.84, as illustrated in Fig. 7c for gates with a power always higher than 50 dB (gates 110, 111, and 112 for 2 μs and gates 111 and 112 for 1 μs). Concerning gate 110 with 1 μs, for which the amplitude is never higher than 40 dB (not shown), the determination criterion is much worse ($R^2 = 0.643$). These determination criteria are summed up in Table 3. Unsurprisingly, a lower pulse width leads to a better location of ground targets, but it does not really impact the refractivity restitution.

2) NONISOLATED GROUND TARGET

The experiment is now performed on a multiple ground target. Nicol et al. (2013) have discussed the problem of spread targets and defined an indicator of these targets. Here we focus on the misbehaving targets, in particular the complex target. The objective is to understand whether the complexity of the target induces a signal complexity.

This is localized in the azimuth 270°, over three range gates (Fig. 7b)—119, 121, and 123—corresponding to distances from the radar of 28.56, 28.80, and 29.04 km, respectively. Regardless of the pulse width, the signal amplitude is always higher than 50 dB for gate 123, most of time between 40 and 55 dB for gate 121, and never higher than 50 dB for gate 119 (not shown).

In this case, the ground target returns are also more spread out and smoother with a pulse of 2 μs than for a pulse of 1 μs (Fig. 7b). Considering the refractivity at each gate, it can be observed that values are similar but not strictly identical, except for the refractivity obtained for gate 121 with a pulse width of 2 μs, which has an atypical behavior (Fig. 7d). These visual observations are confirmed by the determination criterion calculated between the retrieval refractivity and the in situ refractivity, summed up in the Table 4. Indeed, the determination criterion obtained for all different gates with a 1-μs pulse width presents a good quality (Table 4). The determination criterion quality is quickly decreasing for restitution corresponding to a 2-μs pulse width (good for gate 123; bad for gates 121 and 119).

An explanation of these decreases is that, with a 2-μs pulse, the received signal of two ground targets close to each other are mixed. In the present example, the signal received for gate 121 at 2 μs is a mix of the signal from the ground target in gate 121 but also from ground targets from gates 119 and 123. This mixed signal more or less reduces the refractivity measurement quality. So, longer pulses may induce a decrease of the quality and the number of usable ground targets.

To test this hypothesis on our dataset, the distribution of the two quality indices is plotted in Fig. 8, obtained for the two different pulse widths (i.e., $QI_{1\mu s}$ for a 1-μs pulse width and $QI_{2\mu s}$ for a 2 μs). As observed, for ground targets selected around the Nîmes radar (i.e., ~39 000 for 1-μs pulse length and ~44 000 for 2-μs pulse length), the pulse width does not have a strong influence on the QI distribution.

The decreasing pulse width promotes a better location of the ground target and indirectly avoids the mixing

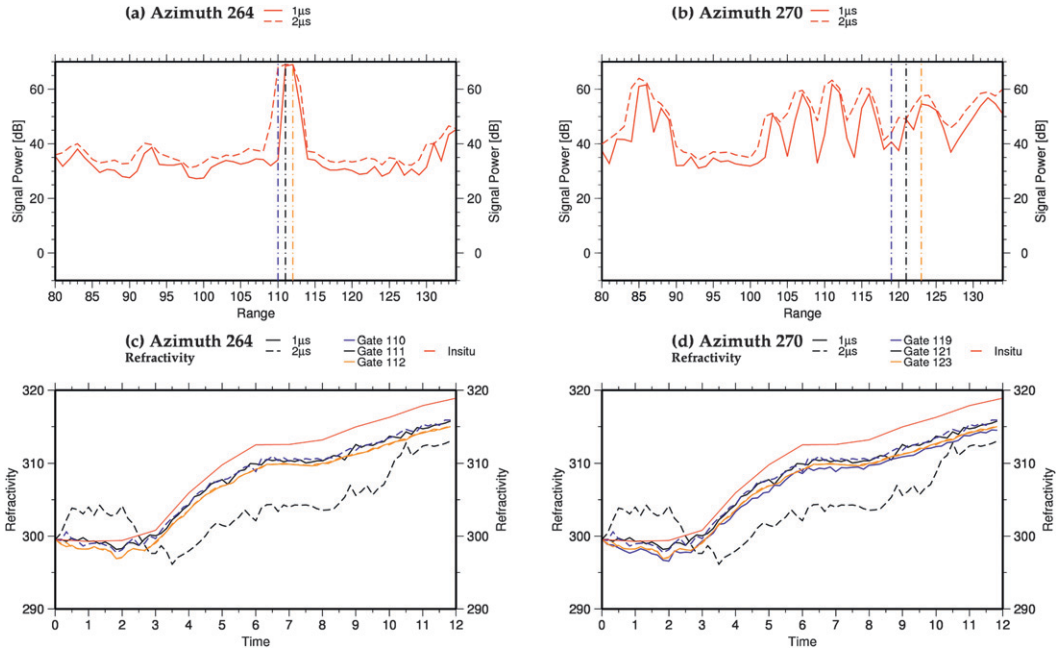

FIG. 7. (top) Range profiles of signal power (dB; red) as a function of range at azimuth (a) 264° and (b) 270°. (bottom) The 12 time series of the refractivity measurement for the in situ parameters (red) and for (c) radar gates 110 (blue), 111 (black), and 112 (orange) in the azimuth 264° and (d) radar gates 119 (blue), 121 (black), and 123 (orange) in the azimuth 270°. Solid and dashed lines indicate respectively a 2-μs and 1-μs transmitter pulse duration on 20 Sep 2012 with the Nîmes radar.

signal between two close ground targets. However, the decrease of pulse duration does not bring a statistically significant improvement of QI distribution for the tested dataset (12 h for the Nîmes S-band radar). This conclusion remains to be verified during the complex propagation condition (convection, turbulent conditions, etc.).

A similar argument can be used in the azimuthal direction. Indeed, for the ARAMIS case, the beam integration in azimuth is 0.5° and leads to an azimuthal resolution of 1.5°, while the beamwidth is 1°. An approach developed by Brown et al. (2002) could be used to reduce the size of the pixel radar azimuth and thus reduce the probability of multiple paths.

b. *Dual polarization*

The ARAMIS network is now mainly composed of dual-polarization radars and the advantages brought out by this technique for rain-rate estimation are described by Bringi and Chandrasekar (2001). The refractivity measurement can be done regardless of the polarization, but the objective here is to evaluate the potential benefit of polarimetric signals to improve refractivity measurements.

As illustrated by Fig. 9, the quality index, defined by Eq. (4) (see section 3b) for a single echo, is not necessarily identical for the two polarizations. Indeed, a ground

TABLE 3. Determination criterion between the in situ refractivity and the retrieval refractivity calculated for one selected isolated target observed on 20 Sep 2012 with the Nîmes radar located at 264° in azimuth and at range gates 110, 111, and 112.

	Gate 110 vs in situ	Gate 111 vs in situ	Gate 112 vs in situ
Determination criterion (R^2) (2-μs pulse length)	0.848	0.849	0.850
Bias (2-μs pulse length)	−0.464	−0.492	−0.528
Determination criterion (R^2) (1-μs pulse length)	0.643	0.843	0.842
Bias (1-μs pulse length)	0.439	−0.565	−0.587

TABLE 4. Determination criterion between the in situ refractivity and the retrieval refractivity calculated for one selected nonisolated target observed on 20 Sep 2012 with the Nîmes radar located at 270° in azimuth and at range gates 119, 121, and 123.

	Gate 119 vs in situ	Gate 121 vs in situ	Gate 123 vs in situ
Determination criterion (R^2) (2-μs pulse length)	0.320	0.360	0.847
Bias (2-μs pulse length)	−0.430	−0.607	−0.435
Determination criterion (R^2) (1-μs pulse length)	0.645	0.863	0.852
Bias (1-μs pulse length)	−0.298	−0.272	−0.485

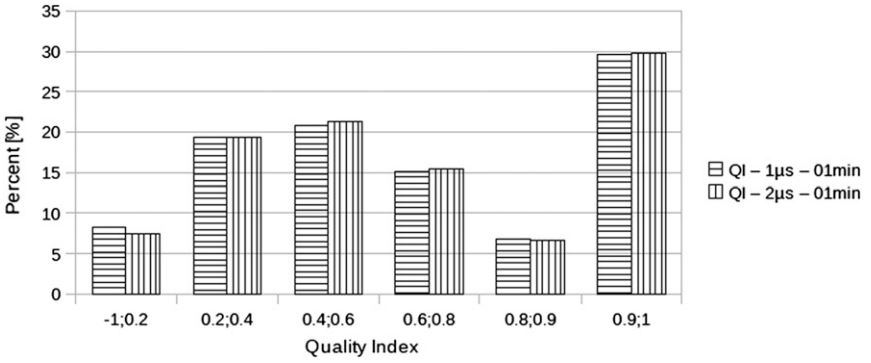

FIG. 8. QI distribution from 20 to 21 Sep 2011 for 12 h with the Nîmes radar. The horizontal hatching corresponds to the $QI_{1\mu s}$ and the vertical hatching to the $QI_{2\mu s}$.

target can have a good QI on the horizontal (or vertical) polarization but a low QI for the vertical (or horizontal) polarization. Through the quality index, the pool of ground target could be classified in two groups:

1) a similar quality index (area I in Fig. 9), and
2) a better quality index on one of the two polarizations (horizontal or vertical; area II in Fig. 9).

Two geographically close pixels, each representing one of the two groups described above, are selected to illustrate the particular behavior of these different populations (Fig. 10). Figure 10a illustrates the first group of ground targets. For this particular pixel, both QI_v and QI_h are equal or higher than 0.978. As it can be observed, the two refractivity restitutions are similar as it is confirmed by good determination criterion and bias (0.994 and −0.105, respectively).

For the second group of ground targets, QIs are significantly different for the two polarizations; this will have consequences on the refractivity measurement. To illustrate that point, we choose one specific pixel having a very good QI (i.e., 0.993) for the horizontal (H) polarization and a relatively low QI for the vertical (V) polarization (i.e., 0.881). As shown by Fig. 10b, this difference leads to a divergence between the two refractivity restitutions. The horizontal refractivity seems correct, while the vertical suffers from several obvious aliasing problems (at time 0, 2, 5, 9, and 15 and also 6 successive aliasings between time 21 and 23; Fig. 10b). This leads to lower determination criterion and bias (0.847 and 6.158, respectively) between the two polarizations.

This difference in behavior can be explained by considering that, inside the scene, each polarization preferably selects the corresponding lines, horizontal or vertical. The horizontal and vertical targets can therefore be significantly different; for example, one can be an isolated target while the other is more complex. This could be used in some way to unalias the worst restitution.

To improve the refractivity measurement, a first possibility is to consider for each pixel only the polarization having the best QI. Distributions of these QIs are shown by Fig. 11. Without having a clear explanation, it is observed that the horizontal polarization gives slightly better results than the vertical polarization, 29% and 26%, respectively. The use of the best QI for each pixel [max (QI_h, QI_v)] leads to an improvement of ground targets availability from 29% to 26%, respectively, with QI_h and QI_v up to 33% for max(QI_h, QI_v) (Fig. 11).

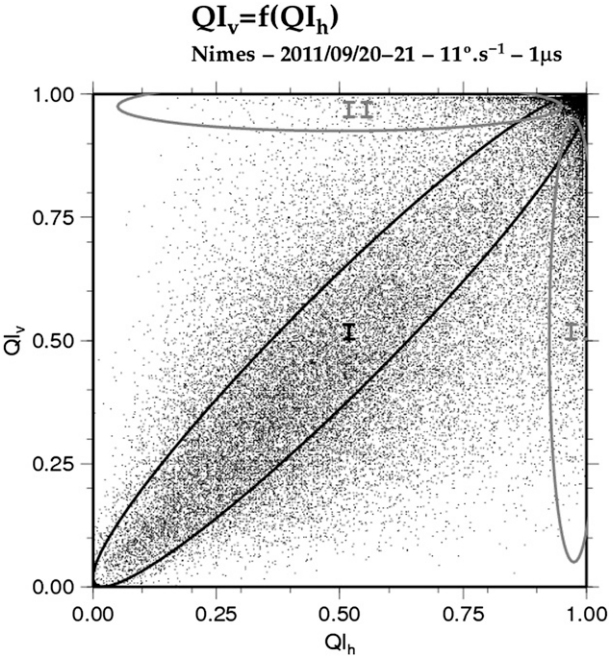

FIG. 9. Scatterplot obtained with the Nîmes radar dataset of the QI calculated for the vertical polarization in function of the quality index calculated for the horizontal polarization. Each ground target is represented by a dot. Area I corresponds to a QI identical between the two different polarizations, while area II corresponds to a better QI on one of the two polarizations.

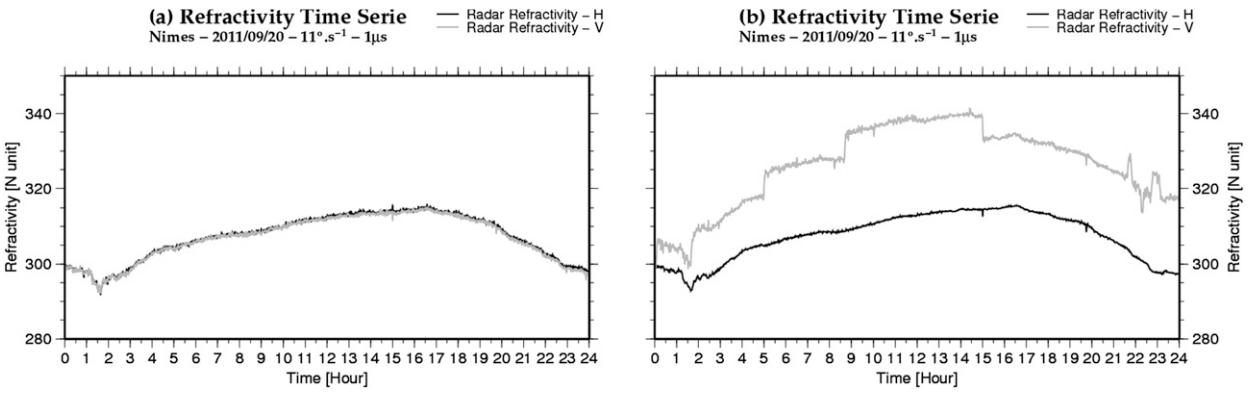

FIG. 10. (a),(b) Time series of the horizontal (gray) and vertical (black) refractivity obtained during 20–21 Sep 2012 with the Nîmes radar. In (a) both targets have a QI higher than 0.978 and in (b) the horizontal ground target has a QI equal to 0.993 and the vertical ground target has a QI equal to 0.881.

To take full advantage of polarimetry, another idea would be to detect the phase changes that are larger than a threshold (for example $\pi/2$) and to replace it with the phase change from the other polarization at this time. To validate this hypothesis, four different QIs have been calculated using the same dataset as for Fig. 2: QI_h obtained with the horizontal phase change [Eq. (4)], QI_v obtained with the vertical phase change [Eq. (4)], max (QI_h, QI_v) (which is the best QI for each pixel), and QI_{hv} obtained with the horizontal and the vertical phase change, defined by the following equation:

$$QI_{hv} = \left[\left(\frac{n_{\pi/2}}{n}\right) \times 2\right] - 1, \qquad (5)$$

where $n_{\pi/2}$ is the number of time with $|\delta\phi_h| \leq \pi/2$ or $|\delta\phi_v| \leq \pi/2$.

The most spectacular result is that QI_{hv} is much larger than QI_h and QI_v separately: while only 26%–30% of the ground echoes stay in the higher-QI class for single polarization, this number increases up to 45% by taking the best of the two polarizations by changing the polarization each time the phase change is larger than $\pi/2$. This result clearly indicates how polarimetry could lead to an improvement in the estimation of refractivity by radar.

The distribution of the different QIs confirms that the dual polarization clearly improves the quality of ground targets and of the refractivity retrieval. This QI_{hv} calculation still has to be improved and tested with different radar frequencies and datasets, particularly as there is a risk that this method of calculation of QI_{hv} [Eq. (5)] could lead to a systematic bias through an underestimation of the phase change.

6. Conclusions

This paper proposes an overview of different solutions to solve some of the major problems inherent to the radar refractivity measurement and to implement them on an operational network.

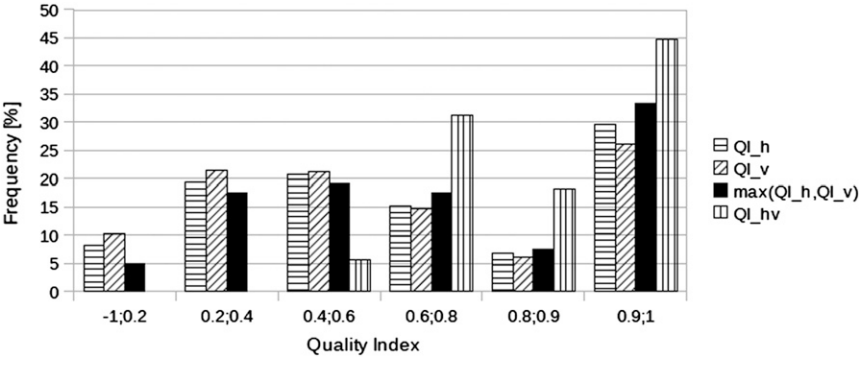

FIG. 11. QI distribution of 40 000 ground targets from 20 to 21 Sep 2011 for 12 h. The horizontal hatching, diagonal hatching, black color, and vertical hatching correspond to QI_h, QI_v, max(QI_h, QI_v), and QI_{hv}, respectively.

For each pixel, a quality index is defined as the percentage of phase change lower than $\pi/2$ during a reference period, typically 6 h in duration. The distribution of QIs over the entire population of ground pixels is clearly bimodal, indicating that only some ground pixels (~25%) are useable for refractivity measurement. Moreover, the QI is useful to evaluate the efficiency of a treatment; on data to which a processing method has been applied, the sharpness of the QI distribution is an indicator of the improvement brought about by this method.

Concerning the sampling time, which is critical to maintain data quality during highly perturbed conditions, we verified that

- the quality of the refractivity measurement is not deteriorated by increasing the antenna rotational speed;
- reducing the sampling time improves the QI distribution sharpness; and
- several signals, returned by different elevation angles, can be mixed together to produce time series having a shorter sampling time. These interlaced signals are only affected by a high-frequency noise, easy to filter out.

Concerning the influence of transmitted pulse duration, we highlighted a few cases in which reducing the transmitted pulse duration could prevent mixing between signals from several targets and consequently could improve the quality of the refractivity measurement. It seems that these cases are relatively rare and not really significant at S band in a global statistic.

As regards the exploitation of polarimetric signals, we showed that the quality index could be very different between the two polarimetric signals. A modified quality index QI_{hv} is defined, which could help to greatly increase the amount of usable signals (from 28% to 45%).

The conclusions made above have been obtained with a relatively short dataset and before going operational, the following tasks must be done:

- Corroborate the bimodal nature of the quality index QI on a larger dataset with more radars and during different meteorological conditions and propagation regimes;
- Verify, through comparison with in situ measurements, that pixels having a good QI actually provide good quality refractivity measurement;
- Verify that the reduction of time sampling actually improves refractivity restitution during perturbed conditions, particularly during deep convection and highly turbulent summer afternoons;
- Test the effect of reducing the pulse duration for shorter wavelengths (C and X band); and
- Verify, with in situ measurements, that the new quality index (i.e., QI_{hv}), by a use of the polarimetric signals, leads to an effective increase of the pixel availability.

Before implementing the different improvements described in this paper, it must be verified that the gains for refractivity do not lead to quality loss for the other variables measured by the radar, like rain rate or radial velocity. Regarding the compatibility of the proposed improvements with conventional parameters, we can say that

- without any negative effects, the combination of several elevations can take better advantage of the operational operating mode;
- the use of polarimetric signals has no negative effect;
- decreasing the pulse duration results in a decrease in the sensitivity of the radar; and
- increasing the rotational speed leads to a decrease of the number of degrees of freedom and therefore some degradation of measurements of the rain rate and radial velocity. However, this will free ''time's radar'' that can be used to reduce the time between successive measurements and thus finally restore the lost degrees of freedom. But this requires a deep change of operating modes, which is not easy to implement.

Acknowledgments. The authors and their organizations thank the European Union, the Provence-Alpes-Côte d'Azur Region, and the French Ministry of Ecology, Energy, Sustainable Development and the Sea for cofinancing the RHYTMME project. Thanks are given to Laurent Périer, who developed the CASTOR2 radar processor. Finally the authors gratefully acknowledge Olivier Caumont for his careful reading of this paper.

REFERENCES

Bean, B. R., and E. J. Dutton, 1968: *Radio Meteorology. Natl. Bur. Stand. Monogr.,* No. 92, National Bureau Standards, 435 pp.

Besson, L., C. Boudjabi, O. Caumont, and J. Parent du Châtelet, 2012: Links between weather phenomena and characteristics of refractivity measured by precipitation radar. *Bound.-Layer Meteor.,* **143,** 77–95, doi:10.1007/s10546-011-9656-7.

Bodine, D., P. L. Heinselman, B. L. Cheong, R. D. Palmer, and D. Michaud, 2010: A case study on the impact of moisture variability on convection initiation using radar refractivity retrievals. *J. Appl. Meteor. Climatol.,* **49,** 1766–1778.

——, and Coauthors, 2011: Understanding radar refractivity: Sources of uncertainty. *J. Appl. Meteor. Climatol.,* **50,** 2543–2560.

Bringi, V. N., and V. Chandrasekar, 2001: *Polarimetric Doppler Weather Radar.* Cambridge University Press, 636 pp.

Brown, R. A., V. T. Wood, and D. Sirmans, 2002: Improved tornado detection using simulated and actual WSR-88D data with enhanced resolution. *J. Atmos. Oceanic Technol.,* **19,** 1759–1771.

Caumont, O., A. Foray, L. Besson, and J. Parent du Châtelet, 2013: Comparisons between observed and simulated weather radar refractivity change. *Bound.-Layer Meteor.,* **148,** 379–397, doi:10.1007/s10546-013-9820-3.

Cheong, B. L., R. D. Palmer, C. D. Curtis, T.-Y. Yu, D. S. Zrnić, and D. Forsyth, 2008: Refractivity retrieval using the phased

array radar: First results and potential for multimission operation. *IEEE Trans. Geosci. Remote Sens.,* **46,** 2527–2537.

Demoz, B., and Coauthors, 2006: The dryline on 22 May 2002 during IHOP_2002: Convective-scale measurements at the profiling site. *Mon. Wea. Rev.,* **134,** 294–310.

Fabry, F., 2004: Meteorological value of ground target measurements by radar. *J. Atmos. Oceanic Technol.,* **21,** 560–573.

——, 2006: The spatial variability of moisture in the boundary layer and its effect on convection initiation: Project-long characterization. *Mon. Wea. Rev.,* **134,** 79–91.

——, C. Frush, I. Zawadski, and A. Kilambi, 1997: On the extraction of near-surface index of refraction using radar phase measurements from ground targets. *J. Atmos. Oceanic Technol.,* **14,** 979–987.

Heinselman, P. L., B. L. Cheong, R. D. Palmer, D. Bodine, and K. Hondl, 2009: Radar refractivity retrievals in Oklahoma: Insights into operational benefits and limitations. *Wea. Forecasting,* **24,** 1345–1361.

Hubbert, J.-C., M. Dixon, S. M. Ellis, and G. Meymari, 2009a: Weather radar ground clutter. Part I: Identification, modeling, and simulation. *J. Atmos. Oceanic Technol.,* **26,** 1165–1180.

——, ——, and ——, 2009b: Weather radar ground clutter. Part II: Real-time identification and filtering. *J. Atmos. Oceanic Technol.,* **26,** 1181–1197.

Montmerle, T., A. Caya, and I. Zawadzki, 2002: Short-term numerical forecasting of a shallow storms complex using bistatic and single-Doppler radar data. *Wea. Forecasting,* **17,** 1211–1225.

Nicol, J., A. Illingworth, T. Darlington, and M. Kitchen, 2013: Improving errors in refractivity retrievals due to transmitter frequency drifts and target position uncertainty. *J. Atmos. Oceanic Technol.,* **30,** 22–39.

Parent du Châtelet, J., and C. Boudjabi, 2008: A new formulation for a signal reflected from a target using a magnetron radar: Consequences for Doppler and refractivity measurements. *Extended Abstracts, Fifth European Conf. on Radar in Meteorology and Hydrology,* Helsinki, Finland, FMI, 0166.

——, P. Tabary, and C. Boudjabi, 2007: Evaluation of the refractivity measurement feasibility with a C-band radar equipped with a magnetron transmitter. Preprints, *33rd Int. Conf. on Radar Meteorology,* Cairns, Australia, Amer. Meteor. Soc., 8B.8. [Available online at https://ams.confex.com/ams/33Radar/webprogram/Paper123581.html.]

——, C. Boudjabi, L. Besson, and O. Caumont, 2012: Errors caused by long-term drifts of magnetron frequencies for refractivity measurement with a radar: Theoretical formulation and initial validation. *J. Atmos. Oceanic Technol.,* **29,** 1428–1434.

Park, S., and F. Fabry, 2010: Simulation and interpretation of the phase data used by the radar refractivity retrieval algorithm. *J. Atmos. Oceanic Technol.,* **27,** 1286–1301.

——, and ——, 2011: Estimation of near-ground propagation conditions using radar ground echo coverage. *J. Atmos. Oceanic Technol.,* **28,** 165–180.

Smith, E. K. J., and S. Weintraub, 1953: The constants in the equation for atmospheric refractive index at radio frequencies. *Proc. IRE,* **41,** 1035–1037.

Sun, J., 2005: Convective-scale assimilation of radar data: Progress and challenges. *Quart. J. Roy. Meteor. Soc.,* **131,** 3439–3463, doi:10.1256/qj.05.149.

Wakimoto, R. M., and H. V. Murphey, 2010: Frontal and radar refractivity analyses of the dryline on 11 June 2002 during IHOP. *Mon. Wea. Rev.,* **138,** 228–240.

Weckwerth, T. M., C. R. Pettet, F. Fabry, S. Park, M. A. Lemone, and J. W. Wilson, 2005: Radar refractivity retrieval: Validation and application to short-term forecasting. *J. Appl. Meteor.,* **44,** 285–300.